Supporting Information

Phosphoproteomic analysis reveals the effects of PilF phosphorylation on Type IV pilus and biofilm formation in *Thermus thermophilus* HB27

Wan-Ling Wu[1,2], Jiahn-Haur Liao[2], Guang-Huey Lin[3], Miao-Hsia Lin[2], Ying-Che Chang[2], Suh-Yuen Liang[2,4], Feng-Ling Yang[2], Kay-Hooi Khoo[1,2,4], and Shih-Hsiung Wu [1,2]*

1. Institute of Biochemical Sciences, College of Life Sciences, National Taiwan University, Taipei, Taiwan

2. Institute of Biological Chemistry, Academia Sinica, Taipei, Taiwan

3. Institute of Microbiology, Immunology and Molecular Medicine, Tzu Chi University, Hualien, Taiwan

4. Core Facilities for Protein Structural Analysis, Academia Sinica, Taipei, Taiwan

Supporting Materials and Methods

Phosphorylation stoichiometry estimation

Overexpressed PilF in *T. thermophilus* HB27 was purified by Ni-affinity chromatography as described in Materials and Methods. The purified His-tagged PilF preparation was split into two parts , i.e., treated or not with calf intestinal alkaline phosphatase (New England BioLabs, MA, USA) for 30 min at room temperature. Identical amounts of phosphoprylated and dephosphorylated PilF proteins were

loaded directly onto a 12.5% acrylamide gel and after SDS-PAGE were stained with Coomassie brilliant blue G-250. Bands corresponding to a molecular mass of about 100 kDa, presumably representing PilF, were excised and in-gel digested with trypsin. The tryptic peptides were desalted for LTQ-Orbitrap Elite hybrid mass spectrometry analysis. The raw MS/MS spectra were processed and quantified using Proteome Discoverer software 1.3 (Thermo Scientific), applying Mascot. Comparisons of the phosphorylation stoichiometry were based on the peak area ratios of non-phosphorylated forms of the target peptides RGGGRLEDTLVQSGK and GGGRLEDTLVQSGK in the phosphatase-treated and untreated samples. The degree of phosphorylation was calculated as [1-(the area ratio untreated / the area ratio treated)] × 100.

LC-MS/MS analysis

Accurate masses of the targeted peptides in high-resolution selected ion monitoring (SIM) mode were collected for quantitation and the MS/MS spectrum of each targeted peptide was used for sequence confirmation. Full scans and five targeted SIM scans followed by a data-dependent CID MS/MS scan with an inclusion list over the entire gradient were set up on the LTQ-Orbitrap Elite. The analysis was performed on a nanoAcquity system (Waters, Milford, MA) connected to an LTQ-Orbitrap Elite hybrid mass spectrometer (Thermo Fisher Scientific, Bremen, Germany) equipped

with a nanospray interface (Proxeon, Odense, Denmark). The peptide mixtures were loaded onto a 75-μm ID, 25-cm length C18 BEH column (Waters, Milford, MA) packed with 1.7-μm particles with a pore size of 130 Å and were separated over 30 min using a segmented gradient from 5% to 40% solvent B (acetonitrile with 0.1% formic acid) at a flow rate of 300 nl/min and a column temperature of 35℃. Solvent A was 0.1% formic acid in water. Full scans (*m/z* 350–1600) were acquired with an AGC target value of 5E5, a resolution of 15,000 at 400 *m/z*, and a maximum ion injection time (IT) of 250 ms. Each target was monitored with a 3-amu isolation window, an AGC target value of 5E4, 15,000 resolution, and a maximum ion IT of 250 ms. A CID MS/MS Scan and data-dependent MS/MS with inclusion lists were used for targeted peptide verification and detection in the linear ion trap, with an AGC target value of 1E4 and a maximum ion IT of 100 ms.

ATPase activity assay

The ATPase activity of PilF and its mutants was determined by ^{31}P-nuclear magnetic resonance (NMR) spectroscopy as described previously (1). The reaction mixtures containing 10 μg purified proteins, 50 mM Tris-HCl (pH 8.0), 150 mM NaCl, 10 mM $MgCl_2$, 2.5 mM ATP, and 10% D_2O were incubated at 37 ^{o}C for 3 days. ^{31}P-NMR spectra were recorded on a Bruker AC 500 spectrometer. Phosphoric acid was used as

an internal reference based on its ^{31}P NMR of 0 ppm, which allowed ^{31}P chemical shifts to be monitored.

Circular dichroism (CD) spectra

The recombinant wild-type PilF and its mutant proteins were analyzed by CD spectroscopy on a JASCO J-715 spectropolarimeter (JASCO, Japan). Protein concentrations were set at 1 μM in a buffer containing 20 mM KH_2PO_4, 100 mM NaF, and 10% glycerol. Data from the far-UV CD spectra were the mean of three accumulations with a 0.1-cm light path. Secondary structure was estimated using three algorithms (CONTIN, SELCON3, and CDSSTR). The results are compiled into in Supporting Information Table S6.

Analytical ultracentrifugation (AUC) analysis

The quaternary structures of recombinant PilF wt and its mutants were analyzed using a Beckman XL-A analytical ultracentrifuge (Beckman Instruments, Fullerton, CA) with an An60Ti rotor. The sedimentation velocity was 20,000 rpm for PilF and its mutants, using standard double-sector centerpieces at 20°C. The UV absorption (280 nm) of the cells was scanned every 4 min for 250 scans. The data were analyzed with SEDFIT (Schuck, 2000). Protein concentrations were set at 120 μM using PBS buffer

SEM of biofilm architecture

Biofilm architecture was imaged using SEM as described previously (2). Briefly,

the dried biofilms were fixed with 2.5% glutaraldehyde in a PBS buffer for 1 h and then postfixed with 0.25% osmium tetroxide in the same buffer for an additional 1 h at room temperature. After their dehydration in a graded (50–100%) series of ethanol solutions by submersion, the samples were subjected to critical point drying (Hitachi HCP-2) and mounted on specimen stubs by gold sputter coating (Ion sputter, Hitachi E-1010). The specimens were stored in a desiccator until SEM (S-4700, Hitachi) observation at 15 kV.

Sugar composition

Sugar composition was determined by GC-MS analyses (Hewlett-Packard Gas Chromatograph HP6890 coupled to an HP5973 Mass Selective Detector). The analytical methods were performed using methanolysis and trimethylsilylation as described previously (3). For the former, each of the dialyzed EPS and monosaccharide standards (both containing arabitol as the internal standard) were treated with a 0.5N methanolic-HCl Kit (Supelco, Bellefonte, PA) at 80℃ for 16 h. Each sample was re-N-acetylated with pyridine/acetic anhydride and trimethylsilylated using the Sylon HTP (HMDS/TMCS/pyridine, 3:1:9) trimethylsilyation reagent (Supelco, PA, USA). After the solvent was removed under a nitrogen stream, the trimethylsilylated derivatives were resolved in n-hexane for GC-MS analysis.

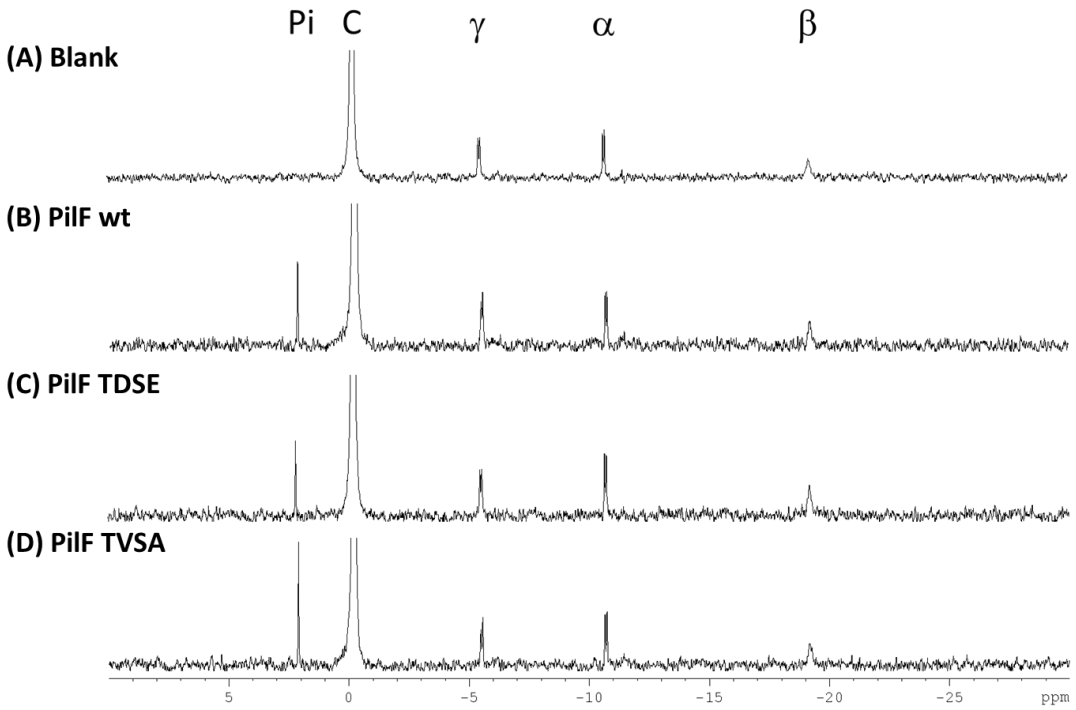

Supporting Information Figure S2. ^{31}P-NMR spectra of ATPase activity from purified PilF wt and mutant PilFs.

The ATPase activities of PilF wt and the double mutants TDSE (T368D/S372E) and TVSA (T368V/S372A) were determined by nucleotide hydrolysis and γ-phosphate release. The blank contained the buffer only. Reactions containing 10 μg of purified protein were incubated at 37 ^{o}C for 3 days. The peaks in the ^{31}P-NMR spectra were, from left to right, inorganic phosphate (P_i) P_i liberated from ATP; an internal control C= 0 ppm; and the γ = 5.6 ppm; α =10.7 ppm, and β = 19.1 ppm of the phosphate groups of ATP.

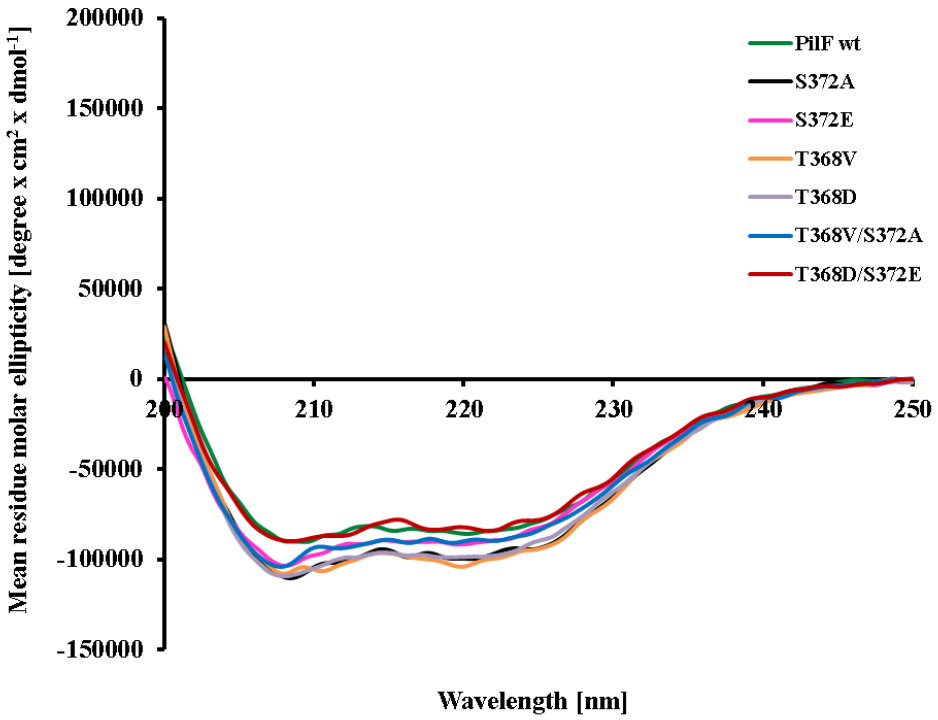

Supporting Information Figure S3. Far-ultraviolet CD spectra of purified wild-type PilF and mutant PilFs.

The secondary structures of purified PilF wt and its mutants were determined from the circular dichroism spectra. The scanning ranges of the CD spectra used for secondary structure determinations were between 250 nm and 200 nm. Scanning was carried out at room temperature and proteins were based on a protein concentration of 1μM.

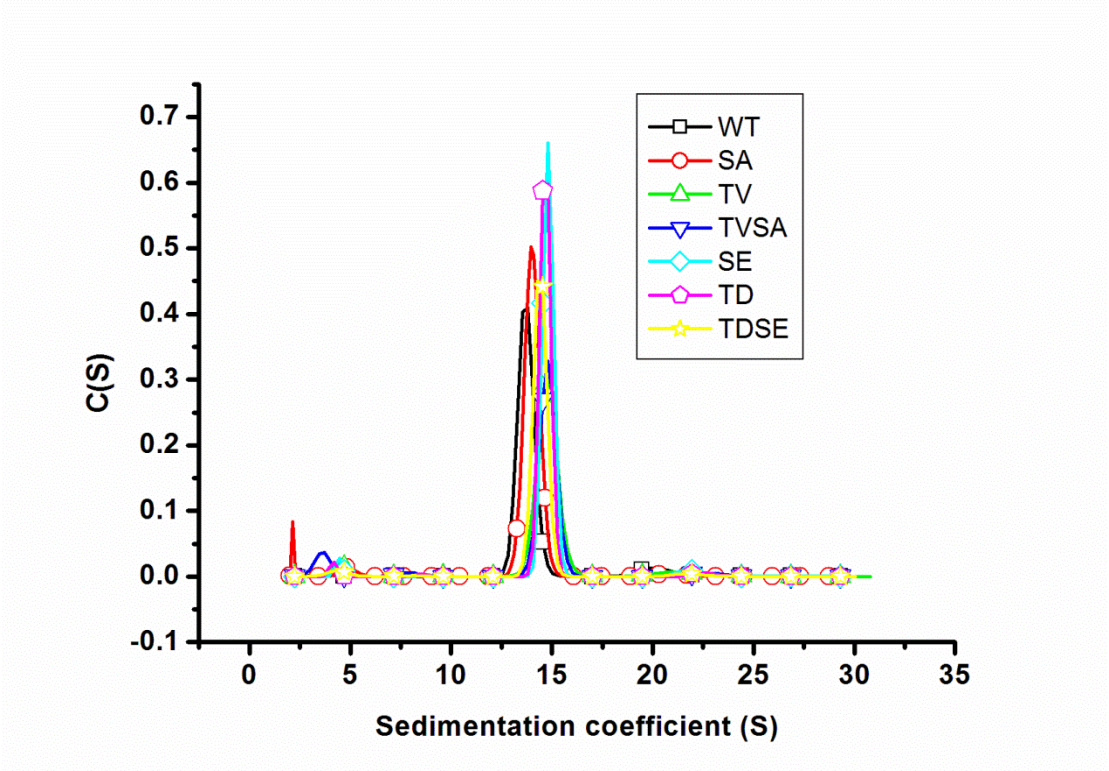

Supporting Information Figure S4. Quaternary structures of purified PilF wt and mutant PilFs.

The quaternary structures of purified PilF wt (WT) and its mutants SA (S372A), TV (T368V), TVSA (T368V/S372A), SE (S372E), TD (T368D), and TDSE (T368D/S372E) were determined by analytical ultracentrifugation analyses. The continuous sedimentation coefficient distribution of the proteins showed a homooligomer of six subunits with a native molecular mass of approximately 595 ± 20 kDa. The total protein concentration was at 120 μM.

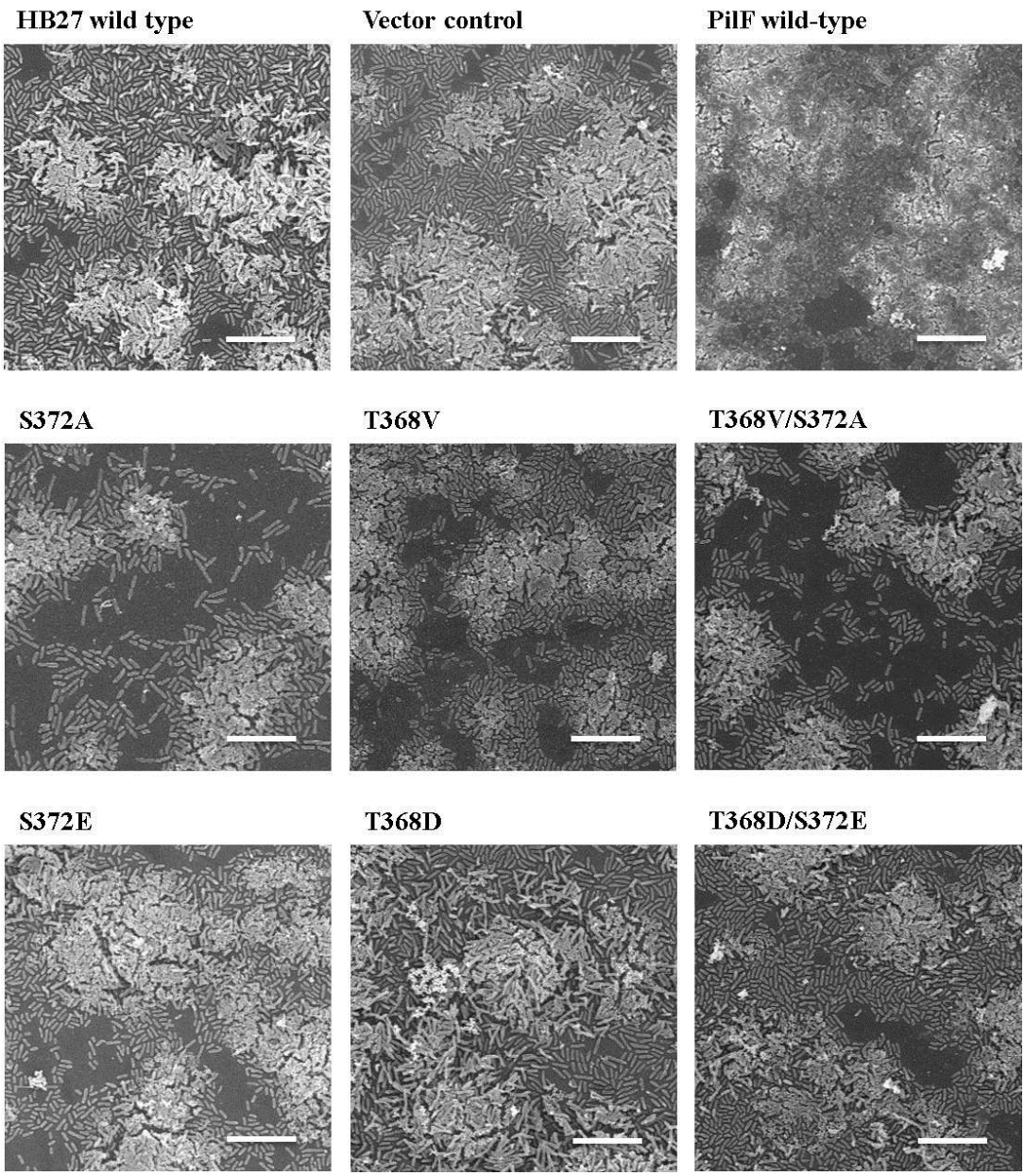

Supporting Information Figure S5. Biofilm architecture of *T. thermophilus* HB27 strains.

The strains were cultured on glass slides in 12-well microtiter plates for 3 h. Biofilm architecture was captured by SEM. Scale bars represent 10 μm.

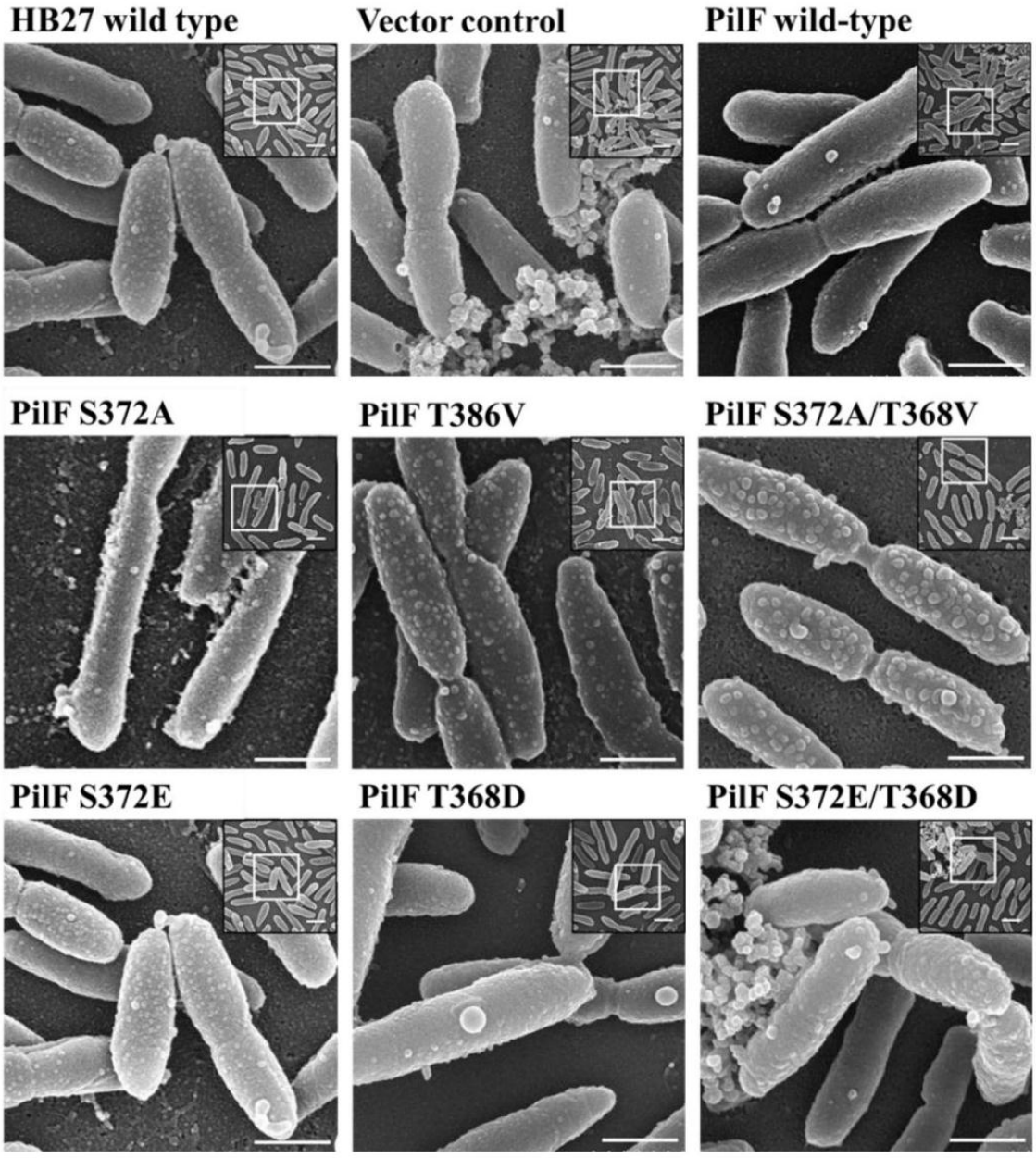

Supporting Information Figure S6. Biofilm attachment of *T. thermophilus* HB27 strains.

The strains were cultured on glass slides in 12-well microtiter plates for 3 h. The initial attachment of the biofilm cells was captured by SEM. Region (scale bar 1 μm) from which the main image was selected and magnified (scale bar 0.5 μm).

Reference

1. Liao, J. H., Kuo, C. I., Huang, Y. Y., Lin, Y. C., Yang, C. Y., Wu, W. L., Chang, W. H., Liaw, Y. C., Lin, L. H., Chang, C. I., and Wu, S. H. (2012) A Lon-like protease with no ATP-powered unfolding activity. *PLoS One* 7, e40226

2. Kolari, M., Schmidt, U., Kuismanen, E., and Salkinoja-Salonen, M. S. (2002) Firm but slippery attachment of *Deinococcus geothermalis*. *J Bacteriol* 184, 2473-2480

3. Yang, F.-L., Lu, C.-P., Chen, C.-S., Chen, M.-Y., Hsiao, H.-L., Su, Y., Tsay, S.-S., Zou, W., and Wu, S.-H. (2004) Structural determination of the polar glycoglycerolipids from thermophilic bacteria *Meiothermus taiwanensis*. *European Journal of Biochemistry* 271, 4545-4551